

This article was downloaded by:

On: 26 January 2011

Access details: *Access Details: Free Access*

Publisher *Taylor & Francis*

Informa Ltd Registered in England and Wales Registered Number: 1072954 Registered office: Mortimer House, 37-41 Mortimer Street, London W1T 3JH, UK



## Liquid Crystals

Publication details, including instructions for authors and subscription information:

<http://www.informaworld.com/smpp/title~content=t713926090>

### Grating coupled liquid crystal waveguide

G. P. Bryan-Brown<sup>ab</sup>; J. R. Sambles<sup>a</sup>; K. R. Welford<sup>b</sup>

<sup>a</sup> Thin Film and Interface Group, Department of Physics, University of Exeter, Exeter, Devon, England

<sup>b</sup> Defence Research Agency, Worcestershire, England

**To cite this Article** Bryan-Brown, G. P. , Sambles, J. R. and Welford, K. R.(1993) 'Grating coupled liquid crystal waveguide', *Liquid Crystals*, 13: 5, 615 – 621

**To link to this Article:** DOI: 10.1080/02678299308026334

**URL:** <http://dx.doi.org/10.1080/02678299308026334>

PLEASE SCROLL DOWN FOR ARTICLE

Full terms and conditions of use: <http://www.informaworld.com/terms-and-conditions-of-access.pdf>

This article may be used for research, teaching and private study purposes. Any substantial or systematic reproduction, re-distribution, re-selling, loan or sub-licensing, systematic supply or distribution in any form to anyone is expressly forbidden.

The publisher does not give any warranty express or implied or make any representation that the contents will be complete or accurate or up to date. The accuracy of any instructions, formulae and drug doses should be independently verified with primary sources. The publisher shall not be liable for any loss, actions, claims, proceedings, demand or costs or damages whatsoever or howsoever caused arising directly or indirectly in connection with or arising out of the use of this material.

## Grating coupled liquid crystal waveguide

by G. P. BRYAN-BROWN\*† and J. R. SAMBLES

Thin Film and Interface Group, Department of Physics, University of Exeter,  
Exeter, Devon EX4 4QL, England

and K. R. WELFORD

Defence Research Agency, Malvern, Worcestershire WR14 3PS, England

(Received 29 October 1992; accepted 1 February 1993)

A waveguide consisting of a thin ( $<1\ \mu\text{m}$ ) layer of nematic liquid crystal sandwiched between two parallel aligned gratings is described. Grating coupling to guided modes is demonstrated by monitoring the reflection and transmission from the cell as a function of incident angle. A reduced birefringence is seen compared to the bulk case which is explained in terms of disordered regions of liquid crystal close to the grating surfaces. The movement of guided modes under electrical bias is shown and time resolved experiments demonstrate high contrast switching with rise times as fast as  $18\ \mu\text{s}$ .

### 1. Introduction

Corrugated multilayer structures are the subject of much research due to the wide variety of applications. Such structures may be used to couple light efficiently into waveguide modes [1] for use as narrow spectral filters [2] or to induce non-linearity in the waveguide properties leading to bistability [3]. To make a tunable filter or a switch we need a waveguide whose optical properties can be perturbed either by an applied electric field or by the optical beam itself. In the former case liquid crystals or electrooptic polymers have been used, but each has its problems. Polymers show small changes in refractive index and are generally used in long ( $\sim 1\ \text{cm}$ ) Mach Zehnder interferometers [4]. Aligned liquid crystal cells can provide a much larger refractive index change but lack speed. By constructing thinner liquid crystal cells, the switching time (which is proportional to cell thickness squared [5]) may be decreased but with the penalty that switching contrast is lost. However, using waveguide modes to increase the contrast, thin liquid crystal cells may be used as high speed, high contrast optical switches.

In this paper we describe a waveguide which is constructed using two diffraction gratings and E7 nematic liquid crystal (obtained from Merck Ltd, Poole, England). The properties of the cell are examined by recording reflection and transmission versus angle under electrical bias. Switching speeds are assessed by time resolved reflectivity studies.

### 2. Experimental

Diffraction gratings used in this study are made using a standard interferographic technique. ITO coated glass substrates ( $238\ \Omega/\square$ ) are cleaned and spin coated at 2000–3000 rpm with AZ 1350 photoresist. The photoresist is dried in an oven at  $60^\circ\text{C}$  for 30 min and then exposed to interfering beams from an argon ion laser operating at 457.9 nm. Once exposed, the sample is developed in microposit developer for 30 s leaving a sinusoidal grating profile in the resist.

\* Author for correspondence.

† Present address: Defence Research Agency, Malvern, Worcestershire WR14 3PS, England.

Such a grating would be inefficient at coupling incident light to waveguide modes when in contact with the liquid crystal as the difference in refractive index between the photoresist and the liquid crystal is low. To increase the difference a 100 nm layer of  $\text{MgF}_2$  ( $n=1.38$ ) is thermally evaporated on to the photoresist. This layer serves a double purpose as it also protects the photo resist from being dissolved by the liquid crystal.

To construct the waveguide, two gratings are placed face to face with the grating grooves parallel. A high degree of parallelism is obtained by making small adjustments to one of the gratings while viewing the Moiré interference fringe pattern in the overlapping diffracted beams. The cell is then capillary filled at room temperature with nematic liquid crystal E7. This liquid crystal is chosen as it has well-characterized properties and is convenient to use. After filling, the cell is clamped tightly to give a liquid crystal thickness of  $\sim 0.7 \mu\text{m}$ . No spacers are present in the cell so the thickness is primarily dependent on the amount of force applied. Figure 1 shows a schematic of the configuration.

The waveguide is first characterized by recording the reflection and transmission versus angle of both p-polarized (TM) radiation and s-polarised (TE) radiation from a He-Ne laser ( $\lambda = 632.8 \text{ nm}$ ). Data are taken under electrical bias by applying a 5 kHz AC voltage between the two ITO layers. This frequency is chosen to avoid beating effects with the 1.7 kHz modulation that is applied to the optical beam for phase sensitive detection purposes. Time resolved data are also recorded by applying short (1 ms) DC pulses to the cell while monitoring the reflectivity at a fixed angle with a fast ( $\tau \sim 1 \mu\text{s}$ ) photodiode. The duty cycle of the applied pulses was kept below 5 per cent to minimize heating of the cell.

Once all the data have been taken, the cell is dismantled, cleaned and each grating surface is coated with an opaque layer of silver to allow grating characterization by the excitation of surface plasmon polaritons. This method has been shown [6] to be an accurate probe of both groove depth and pitch.

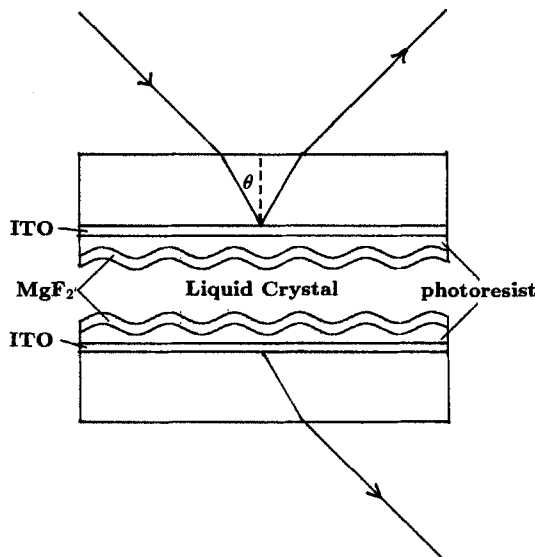


Figure 1. Waveguide structure consisting of E7 liquid crystal sandwiched between two parallel aligned gratings.

### 3. Results

Figure 2 shows the s-polarized transmission and reflection from a liquid crystal waveguide for applied voltages of 0.0 V, 3.0 V and 6.0 V (rms). The angle range refers to the internal angle inside the glass (shown as  $\theta$  in figure 1) and the data have been corrected for reflection at the air/glass interfaces. Each scan clearly shows two TE guided mode resonances which appear as peaks in the normally low reflectivity or as dips in the normally high transmissivity. Excitation of such modes occurs at angles of incidence,  $\theta$ , such that

$$nk \sin \theta + k_g = k_{GM}, \quad (1)$$

where  $n$  is the index of the bounding media (glass),  $k_g$  is the reciprocal grating vector,  $k = 2\pi/\lambda$  and  $k_{GM}$  is the guided mode propagation wavevector. For zero volts the TE<sub>1</sub> mode is excited at 26.70° and the TE<sub>0</sub> mode is excited at 31.26°. Fitting the angles of these modes to rigorous grating theory [7] allows the liquid crystal waveguide layer to be characterized. In this case the layer has a thickness of 0.71  $\mu\text{m}$  and a refractive index of 1.677. For parallel alignment the TE mode positions should only be dependent on  $n_{\parallel}$  which for E7 at room temperature is 1.727. The fact that the observed index is less than this suggests that the liquid crystal director may have some pretilt with respect to the alignment surface. The average tilt angle,  $\phi$ , between the nematic director and the substrate plane necessary to account for the measured refractive index can be estimated from [8]

$$n = \frac{n_{\parallel} n_{\perp}}{\sqrt{(n_{\parallel}^2 \sin^2 \phi + n_{\perp}^2 \cos^2 \phi)}}. \quad (2)$$

Using the observed value for  $n$  and 1.5182 for  $n_{\perp}$ , we obtain  $\phi = 27^\circ$ . A reduced birefringence has been previously noted in a thin MBBA cell aligned by square wave gratings [9] which was interpreted as implying a tilt angle of 23°. There is, however, an alternative explanation for the reduced birefringence, and that is that the liquid crystal in the vicinity of the grating grooves is disordered and so appears isotropic. This effect has been seen before for thin cells of E7 [10] where it was found that these disordered

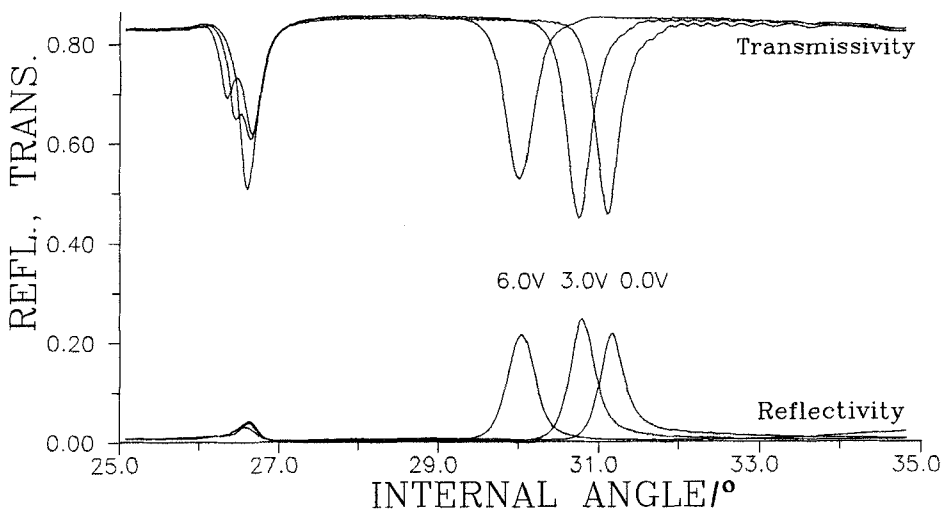


Figure 2. Transmissivity and reflectivity of s-polarized light as a function of internal angle from the liquid crystal cell under a bias of 0.0 V, 3.0 V and 6.0 V (rms, 5 kHz).

regions extend a distance of  $0.19 \mu\text{m}$  from each surface. Therefore, for the  $0.71 \mu\text{m}$  cell studied here, only the central  $0.33 \mu\text{m}$  is likely to be aligned. In this study, by exciting guided modes, we may distinguish between the two possible explanations.

The reflectivity of p-polarized light from the sample for applied voltages of  $0.0 \text{ V}$ ,  $3.0 \text{ V}$  and  $6.0 \text{ V}$  is shown in figure 3. The mode at  $26.11^\circ$  is the  $\text{TM}_0$  guided mode, but the mode at  $30.81^\circ$  is the  $\text{TE}_0$  mode which has become a mixed mode [11] due to a finite tilt angle. The mode is only clearly defined in the  $6.0 \text{ V}$  scan and so we may conclude that the tilt angle is negligible for  $0.0 \text{ V}$ . If the explanation for the reduced  $n_{\parallel}$  refractive index measured were a finite surface director tilt angle, then the  $\text{TE}_0$  mixed mode would be observed at  $0.0 \text{ V}$ . Therefore, the reduced birefringence seen here, and possibly the results in [9] are due to disorder in the surface regions as opposed to a finite tilt angle. The angle of the  $\text{TM}_0$  mode in figure 3, when fitted to theory, corresponds to an index of  $n = 1.556$  (assuming the previous value for cell thickness). TM modes should only be influenced by  $n_{\perp}$  ( $1.5182$  for E7 at  $25^\circ\text{C}$ ) and so this guided mode also shows a reduced birefringence in the cell. Thus the cell can be qualitatively modelled as consisting of two disordered surface regions with a central region that has no pretilt but exhibits small tilt under bias. The presence of disorder in the cell is also possibly implied by the fact that the nematic to isotropic transition temperature for this cell was found to be  $2.1^\circ\text{C}$  lower than that measured for thick ( $\sim 5 \mu\text{m}$ ) cells.

The threshold voltage was found by detecting the onset of the guided mode shift with increasing voltage. In this case a value of  $1.55 \text{ V}$  was found. Theoretically the threshold voltage is given by [12]

$$V_0 = \pi \sqrt{\left(\frac{K_{11}}{\epsilon_0 \Delta \epsilon}\right)}. \quad (3)$$

For E7,  $K_{11} = 11.7 \times 10^{-12} \text{ N}$  and  $\epsilon_0 \Delta \epsilon = 1.27 \times 10^{-10} \text{ F m}^{-1}$  at room temperature and so equation (3) gives a value of  $0.954 \text{ V}$ . Therefore, the measured value for this cell is enhanced compared to theory. This is due to the voltage that is dropped across the photoresist and  $\text{MgF}_2$  layers.

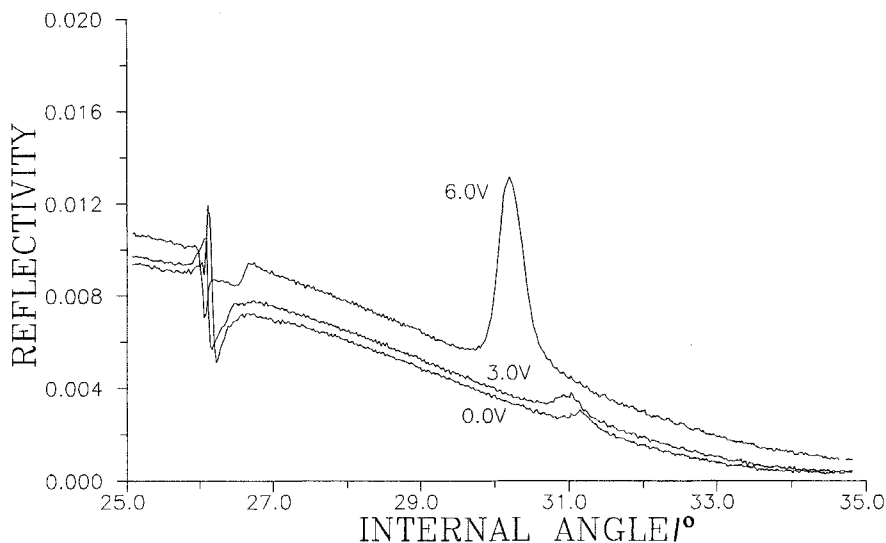


Figure 3. Reflectivity of p-polarized light as a function of angle under applied bias.

It is of interest to calculate the alignment energy of the grating surface. Berreman [13] described a surface by  $z = A \sin qx$  and showed that the energy difference per unit area between parallel and perpendicular orientations of the liquid crystal with respect to the grating grooves is given by

$$U = \frac{1}{4} K_{11} A^2 q^3. \quad (4)$$

The diffraction gratings used here were characterized by first dismantling the liquid crystal cell and coating the grating surfaces with silver by vacuum evaporation. Surface plasmon resonances were then optically excited on the silver surfaces and accurately fitted by rigorous grating theory. Both the gratings were found to have a pitch of  $743.2 \pm 0.5$  nm and a peak to trough groove depth of  $70.6 \pm 0.4$  nm. Therefore, for E7, equation (4) gives an energy difference of  $2.20 \times 10^{-6} \text{ J m}^{-2}$ . For rubbed polymer surfaces, the alignment is provided by grooves which are usually found to have a pitch of  $\sim 20$  nm and a depth of  $\sim 2.0$  nm [13], and hence in this case equation (4) gives an energy difference of  $1.81 \times 10^{-4} \text{ J m}^{-2}$ . It is perhaps surprising that the gratings used here give such good alignment having  $\sim 80$  times less alignment energy than rubbed surfaces. In fact further tests revealed that gratings with half the groove depth ( $\sim 350$  nm) (and hence a quarter of the alignment energy) still produce good uniform alignment of E7.

The switch speed of the cell was measured by fixing the angle of incidence at the  $\text{TE}_0$  guided mode resonance and measuring the reflectivity during the application of 1.00 ms DC pulses separated by 22.0 ms. DC pulses were used as high frequency AC was found to be shorted out due to the capacitance of the sample. Figure 4 shows the applied voltage pulse and the reflectivity response for 3.50 V (curve A) and 13.28 V (curve B) pulses. Switch-on and switch-off times are measured and plotted as a function of voltage as shown in figure 5. The growth time for a Fréedericksz deformation for small deviations from the initial orientation is given by [5]

$$\frac{1}{\tau_{\text{on}}} = \frac{\pi^2 K_{11}}{d^2 \gamma_1 (1 - \alpha_s)} \left[ \left( \frac{V}{V_0} \right)^2 - 1 \right], \quad (5)$$

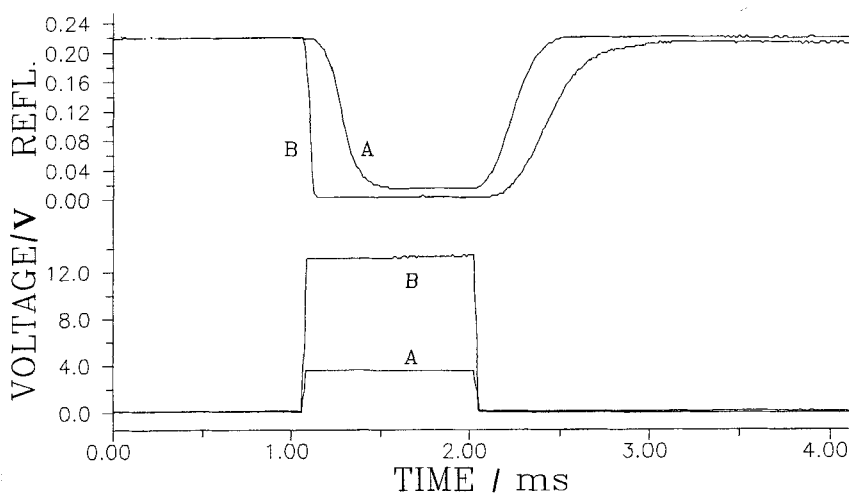


Figure 4. Time resolved data showing applied DC pulses (lower traces) and the reflectivity response of the liquid crystal cell (upper trace). A, 3.50 V; B, 13.28 V.

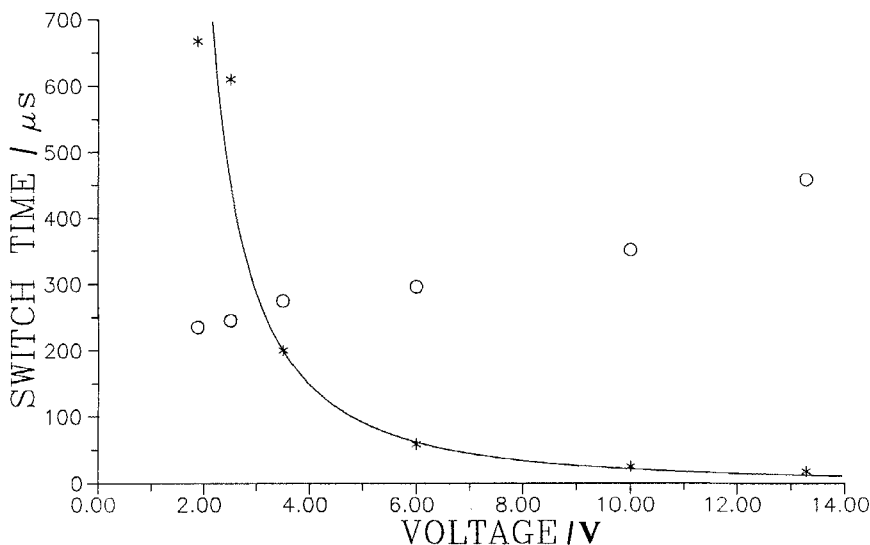


Figure 5. Switch-on (stars) and switch-off (circles) time as a function of the applied DC voltage. The theoretical fit to the former is obtained using equation (5).

where  $V$  is the applied voltage,  $V_0$  is the threshold voltage,  $d$  is the cell thickness,  $\gamma_1$  is the rotational viscosity and  $(1 - \alpha_s)$  is a correction for backflow effects which is close to 1 for a splay deformation. The solid line in figure 5 is a fit to data using the above equation with  $V_0$  set to 1.24 V and  $(\pi^2 K_{11}/d^2 \gamma_1 (1 - \alpha_s))$  set to  $726 \text{ s}^{-1}$ . Using known values for  $K_{11}$  and  $d$  assuming that  $(1 - \alpha_s) \approx 1$ , we get a value of  $0.32 \text{ Pa s}$  for  $\gamma_1$  which is in fairly good agreement with the quoted value of  $0.40 \text{ Pa s}$  ([14]). The switch-off time depends on the liquid crystal relaxation and is given by [5]:

$$\frac{1}{\tau_{\text{off}}} = \frac{\pi^2 K_{11}}{d^2 \gamma_1 (1 - \alpha_s)}. \quad (6)$$

Using the quoted value for  $\gamma_1$ , equation (6) predicts a switch-off time of  $830 \mu\text{s}$ . The fact that the observed  $\tau_{\text{off}}$  depends on voltage is almost certainly due to charge migration during the application of the pulse which sets up a reverse field and hence slows down the relaxation. However, even the high voltage relaxation is faster than the value calculated above which is not presently understood.

#### 4. Discussion

In this work, parallel aligned gratings have produced good alignment of E7 liquid crystal. Examination of the cell between crossed polarizers showed uniform alignment and extinction angles across the entire grating surface ( $1.5 \text{ cm} \times 1.5 \text{ cm}$ ). The extinction angles coincided with the azimuthal angles parallel and perpendicular to the grating groove direction. Simple calculations have shown that the alignment energy of such gratings is small compared to rubbed polymers. Other possible alignment processes such as alignment due to the  $\text{MgF}_2$  alone or flow alignment during the cell filling were discounted by control experiments.

Examination of guided modes confirmed that the director was aligned parallel and not perpendicular to the groove direction and also showed reduced birefringence in the cell which could only be due to disordered surface regions (supporting the conclusions of [10]).

Time resolved experiments showed that even a thin cell ( $0.71\ \mu\text{m}$  in this case) can take full advantage of the  $d^2$  dependence of the switch-on time. The fastest time recorded was  $18\ \mu\text{s}$  with an applied DC pulse of  $13.28\ \text{V}$ . This is probably the fastest switch time seen with a nematic and could easily be improved by using faster liquid crystals such as ferroelectrics. Also the relatively slow switch-off time may be speeded up by employing two-frequency excitation using a material whose dielectric anisotropy changes sign in the  $100\text{--}500\ \text{kHz}$  range.

The switching speeds make the grating waveguide very attractive as a switching element and the switching contrast in reflection (shown in figure 4) is good ( $> 50:1$ ). However, the insertion loss needs to be improved by increasing the coupling efficiency to the guided modes. Experiments carried out with similar waveguides filled with high index fluid (diiodomethane,  $n=1.75$ ) have already shown reflectivity peaks of 75 per cent while still maintaining a very low off-resonance level. The reduced efficiency ( $\sim 22$  per cent) seen in the liquid crystal waveguide can be attributed to the smaller index contrast between the liquid crystal and the  $\text{MgF}_2$  and also the increased optical scatter due to the disordered surface regions. The latter effect also explains why the modes are broader than expected. Therefore future waveguides must incorporate liquid crystals which can be two-frequency driven, have a high  $n_{\parallel}$  and also suffer less disorder in the surface regions. Such waveguides will be fast optical switches which may be used in reflection or transmission.

G. B. B. acknowledges D.R.A. (Malvern) for their support of a postdoctoral fellowship. The authors also acknowledge fruitful discussions with Dr J. C. Jones (D.R.A., Malvern).

### References

- [1] CHUANG, S. L., and KONG, J. A., 1983, *J. opt. Soc. Am.*, **73**, 669.
- [2] GALLATIN, G. M., 1987, *Proc. S.P.I.E.*, **815**, 158.
- [3] AVRUTSKII, I. A., and SYCHUGOV, V. A., 1990, *Sov. J. quant. Electron.*, **20**, 856.
- [4] MOHLMANN, G. R., and HORSTHUIS, W. H. G., 1990, *Proc. S.P.I.E.*, **1337**, 215.
- [5] SCHIEKEL, M., FAHRENSCHON, K., and GRULER, H., 1975, *Appl. Phys.*, **7**, 99.
- [6] BRYAN-BROWN, G. P., ELSTON, S. J., and SAMBLES, J. R., 1991, *J. mod. Opt.*, **38**, 1181.
- [7] CHANDEZON, J., DUPUIS, M. T., CORNET, G., and MAYSTRE, D., 1982, *J. opt. Soc. Am.*, **72**, 839.
- [8] DEULING, H. J., 1972, *Molec. Crystals liq. Crystals*, **19**, 123.
- [9] FLANDERS, D. C., SHAVER, D. C., and SMITH, H. I., 1978, *Appl. Phys. Lett.*, **32**, 597.
- [10] WU, S. T., and EFRON, V., 1986, *Appl. Phys. Lett.*, **48**, 624.
- [11] ELSTON, S. J., SAMBLES, J. R., and CLARK, M. G., 1989, *J. mod. Opt.*, **36**, 1019.
- [12] ANEVA, N., PETROV, A. G., SOKEROV, S., and STOYLOV, S. P., 1989, *Molec. Crystals liq. Crystals*, **60**, 1.
- [13] BERREMAN, D., 1972, *Phys. Rev. Lett.*, **28**, 1683.
- [14] TARRY, H. A., 1975, *Electronics Lett.*, **11**, 339.